Supporting Information for "Ingestible Functional Magnetic Robot with Localized Flexibility (MR-LF)"

Taylor E. Greenwood[1], Henry Cagle[1], Benson Pulver[1], On Shun Pak[1], and Yong Lin Kong[1]

[1]Affiliation not available

September 9, 2022

Abstract

This Supporting Information includes information regarding the magnetic field of the actuator magnet, MR-LF-S (which has the same geometry as MR-LF and a soft compartment), and a table comparing MR-LF to other small-scale, flexible magnetic crawler robots.

Corresponding author email: *yong.kong@utah.edu*

Body flexibility of MR-LF-S

As noted in the text, the closeness of the MR-DF and MR-LF curves indicates that the method of localizing flexibility was successful at reducing the bending region length while preserving body flexibility. The data for the MR-LF-S (shown in **Figure 2**A) has a higher amplitude, indicating higher flexibility. Further, the flat section at the top of the MR-LF-S curve appears to be a result of the foot contacting the compartment. Indeed, images show the MR-LF-S foot contacting the body at the maximum and minimum flexion (indicated by red arrows in Figure 2B), which may cause undesirable effects in locomotion. Because the geometry of the flexure was the same between MR-LF and MR-LF-S models, the additional bending in the MR-LF-S model could be due to bending in the soft compartment and an expected difference in wall effects compared to MR-LF.

A comparison of locomotion results between MR-LF and MR-LF-S with the same mass show that MR-LF-S exhibited a slightly higher initial speed (4%) at $y_a = 11$ cm, slower initial speed (47%) at $y_a = 15$ cm (**Figure 3**A), and a longer period of inhibited gait for locomotion of one trial at $y_a = 10$ cm (indicated by right-pointing arrow in Figure 3B), which was not included in d_{a*}. The data in Figure 3B also show that the mean of data within d_{a*} was close between robots (MR-LF: 14.22 cm, MR-LF-S: 14.19 cm), indicating that the robots stopped locomotion at a similar location, likely as a result of their equal mass. Additionally, the MR-LF-S d_{a*} had a larger standard deviation (MR-LF: 0.23 cm, MR-LF-S: 0.75 cm), indicating MR-LF-S had more variability in locomotion distance after 40 steps. From these results, we see that a robot with a soft compartment (i.e., MR-LF-S) exhibits comparable locomotion to a robot with a rigid compartment (i.e., MR-LF), where differences between the designs can be attributed to the additional flexibility (increase of 61% in maximum and 48% in minimum foot flexion) exhibited by the soft body configuration. These observations can be applied in future applications when, for example, fabricating entirely-soft robots by magnetic 3D printing.

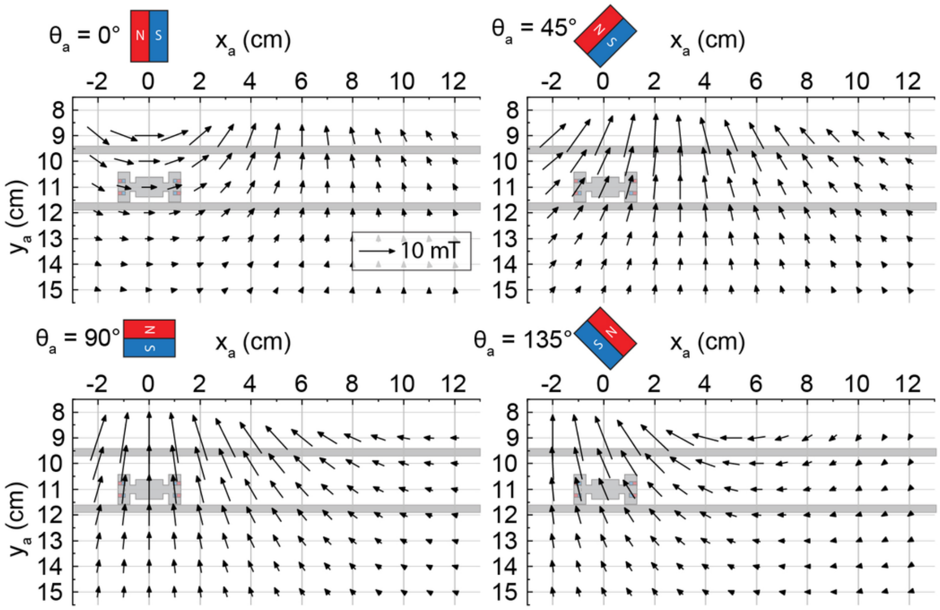

Figure 1: Experimentally measured magnetic field at four actuator magnet orientations (shown above plots). Cross-sections of the MR-LF robot and channel are included to aid visualization.

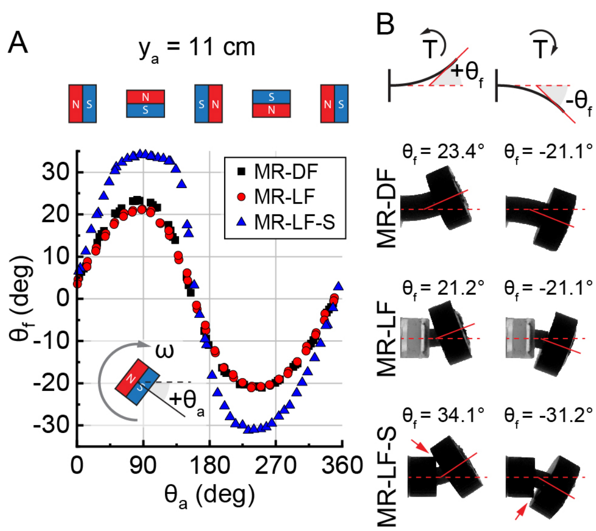

Figure 2: Comparison of body flexibility between the MR-DF, MR-LF, and MR-LF-S designs. (**A**) Foot flexion angle (ϑ_f), as a function of actuator magnet orientation (ϑ_a) for half-robots at x = 0, $y_a = 11$ cm. The amplitude of data sets indicates the foot's flexibility. (**B**) Images of half-robots at their maximum (left) and minimum (right) foot flexion. Arrows on MR-LF-S images point to where the foot contacted the compartment.

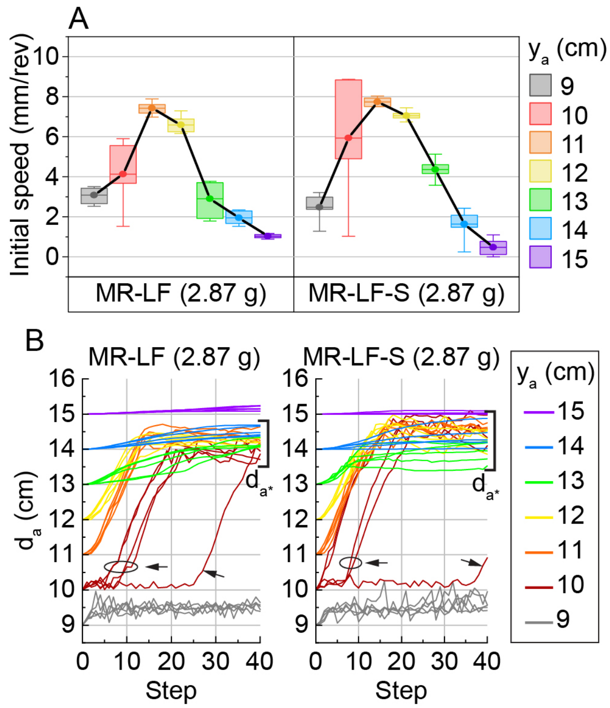

Figure 3: Effect of compartment rigidity on locomotion. (**A**) Initial speed of MR-LF (left) and MR-LF-S (right) with equal mass across y_a offsets (box colors). Boxes show the 25-75% range, whiskers indicate min-max, and mean values are connected by a black line (n = 5). A comparison between plots shows the effect of compartment configuration on speed, where the MR-LF robot has a rigid compartment, and the MR-LF-S has a soft compartment. (**B**) Total actuation distance (d_a) as a function of step number for the MR-LF (left) and MR-LF-S (right) of equal mass across y_a distances (line color). Trials of y_a = 10 to 14 cm converge within a span of d_a (indicated by brackets and denoted d_{a*}) which corresponds to the minimum field strength needed for locomotion.

Row	Reference	Basic robot geometry	Robot magnets	Actuation type	Actuation field motion	Transport cargo	Compartment (location)	Compartment internal volume (mm^3)	Compartment-to-robot volume	Flexibility	Drug release	Incorporated electronics	Body length (mm)	Outer diameter or width (mm)	Gait reported for robot	Max. Avg. speed (mm/s)	Max. Avg. speed (B.L./s)	Gait used in reported speed
1	This work (2.55 g MR-LF	rod with feet	P	D	rotating	Y	Y (in body)	300	17%	L	Y	Y	25	12	run, walk, crawl	13.64	0.55	"run" (crawl-like)
2	This work (MR-DF)	rod with feet	P	D	rotating	N	N	-	-	D	N	N	25	12	run, walk, crawl	13.22	0.53	"run" (crawl-like)
3	1	rod with feet	P	D	rotating	N	N	-	-	D	N	N	20	5	crawl	7.5*	0.38*	crawl
4	2	rod with feet	P	D	rotating	N	N	-	-	D	N	N	30, 14, 25	10, 5, 12	crawl	NR, NR, 8.7	NR, NR, 0.35	crawl
5	3	rod with feet	P	D	rotating	N	N	-	-	D	N	N	24	5	crawl	0.8	0.03	crawl
6	4	rod	P	U	rotating	N	N	-	-	D	N	N	25-30	3	multiple	10.5*	0.42*	tumble
7	5	sheet	M-EC	U	rotating	N	N	-	-	D	N	N	5.9	1.9	swim	100.3	17	swim
8	6	sheet	M-EC	U	various	Y	Y (attached)	2.5x10-2	2.4%*	D	N	N	3.7	1.5	multiple	65.5	17.7	walk
9	7	sheet	M-EC	U	various	N	N	-	-	D	N	N	3.5 (various tested)	1	multiple	1*	0.29*	crawl in fluid
10	8	sheet	M-EC	U	various	Y	N	-	-	D	N	N	6.4	2.5	multiple	2.46	0.38	roll
11	9	sheet	M-EC	U	various	N	N	-	-	D	N	N	6	1	multiple	0.83	0.14	crawl underwater
12	10	sheet	M-EC	U	various	Y	Y (attached)	0.58*	36%*	D	Y	N	3.7	1.5	multiple	0.39*, 0.63*, 0.12*	0.1*, 0.17*, 0.03*	roll, crawl, walk
13	11	sheet with legs	M-EC	D	various	Y	N	-	-	D	N	N	17	7	multiple	28.6*	1.68*	walk*
14	12	inchworm	M-EC	D	translating	Y	N	-	-	Other	N	N	40	5	crawl	1.67*	0.04*	inch
15	13	inch-	M-EC	D	trans-	Y	Y (i	9.3	6%	Other	Y	N	40	5	mul-	3.1	0.08	inch

References for Table 1:

1: (Pham and Abbott, 2018)

2: (Pham et al., 2020)

3: (Steiner et al., 2022)

4: (Bhattacharjee et al., 2020)

5: (Diller et al., 2014)

6: (Hu et al., 2018)

7: (Ren et al., 2021)

8: (Xu et al., 2022)

9: (Du et al., 2020)

10: (Wu et al., 2022)

11: (Lu et al., 2018)

12: (Joyee and Pan, 2019a)

13: (Joyee and Pan, 2019b)

14: (Kim et al., 2013)

15: (Ze et al., 2022a)

16: (Ze et al., 2022b)

17: (Miyashita et al., 2016)

18: (du Plessis d'Argentre et al., 2018)

19: (Kim et al., 2011)

20: (Nam et al., 2014)

References

Anuruddha Bhattacharjee, Louis William Rogowski, Xiao Zhang, and Min Jun Kim. Untethered Soft Millirobot with Magnetic Actuation. In *2020 IEEE International Conference on Robotics and Automation (ICRA)*, pages 3792–3798. IEEE, may 2020. ISBN 978-1-7281-7395-5. doi: 10.1109/ICRA40945.2020.9197202. URL https://ieeexplore.ieee.org/document/9197202/.

Eric Diller, Jiang Zhuang, Guo Zhan Lum, Matthew R. Edwards, and Metin Sitti. Continuously distributed magnetization profile for millimeter-scale elastomeric undulatory swimming. *Applied Physics Letters*, 104 (17):174101, apr 2014. ISSN 0003-6951. doi: 10.1063/1.4874306. URL http://aip.scitation.org/doi/10.1063/1.4874306.

Xuemin Du, Huanqing Cui, Tiantian Xu, Chenyang Huang, Yunlong Wang, Qilong Zhao, Yangsheng Xu, and Xinyu Wu. Reconfiguration, Camouflage, and Color-Shifting for Bioinspired Adaptive Hydrogel-Based Millirobots. *Advanced Functional Materials*, 30(10):1909202, mar 2020. ISSN 1616-301X. doi: 10.1002/adfm.201909202. URL https://onlinelibrary.wiley.com/doi/10.1002/adfm.201909202.

Alexis du Plessis d'Argentre, Samuel Perry, Yoshitaka Iwata, Haruna Iwasaki, Eiji Iwase, Assunta Fabozzo, Iain Will, Daniela Rus, Dana D. Damian, and Shuhei Miyashita. Programmable Medicine: Autonomous, Ingestible, Deployable Hydrogel Patch and Plug for Stomach Ulcer Therapy. In *2018 IEEE International Conference on Robotics and Automation (ICRA)*, pages 1511–1518. IEEE, may 2018. ISBN 978-1-5386-3081-5. doi: 10.1109/ICRA.2018.8460615. URL https://ieeexplore.ieee.org/document/8460615/.

Wenqi Hu, Guo Zhan Lum, Massimo Mastrangeli, and Metin Sitti. Small-scale soft-bodied robot with multimodal locomotion. *Nature*, 554(7690):81–85, feb 2018. ISSN 0028-0836. doi: 10.1038/nature25443. URL http://www.nature.com/articles/nature25443.

Erina B. Joyee and Yayue Pan. A Fully Three-Dimensional Printed Inchworm-Inspired Soft Robot with Magnetic Actuation. *Soft Robotics*, 6(3):333–345, jun 2019a. ISSN 2169-5172. doi: 10.1089/soro.2018.0082. URL https://www.liebertpub.com/doi/10.1089/soro.2018.0082.

Erina Baynojir Joyee and Yayue Pan. Multi-material Additive Manufacturing of Functional Soft Robot. *Procedia Manufacturing*, 34:566–573, 2019b. ISSN 23519789. doi: 10.1016/j.promfg.2019.06.221. URL https://linkinghub.elsevier.com/retrieve/pii/S2351978919309515.

S. H. Kim, S. Hashi, and K. Ishiyama. Magnetic Actuation Based Snake-Like Mechanism and Locomotion Driven by Rotating Magnetic Field. *IEEE Transactions on Magnetics*, 47(10):3244–3247, oct 2011. ISSN 0018-9464. doi: 10.1109/TMAG.2011.2143698. URL https://ieeexplore.ieee.org/document/6027705/.

Sung Hoon Kim, Shuichiro Hashi, and Kazushi Ishiyama. Hybrid magnetic mechanism for active locomotion based on inchworm motion. *Smart Materials and Structures*, 22(2):027001, feb 2013. ISSN 0964-1726. doi: 10.1088/0964-1726/22/2/027001. URL https://iopscience.iop.org/article/10.1088/0964-1726/22/2/027001.

Haojian Lu, Mei Zhang, Yuanyuan Yang, Qiang Huang, Toshio Fukuda, Zuankai Wang, and Yajing Shen. A bioinspired multilegged soft millirobot that functions in both dry and wet conditions. *Nature Communications*, 9(1):3944, dec 2018. ISSN 2041-1723. doi: 10.1038/s41467-018-06491-9. URL http://www.nature.com/articles/s41467-018-06491-9.

Shuhei Miyashita, Steven Guitron, Kazuhiro Yoshida, Shuguang Li, Dana D. Damian, and Daniela Rus. Ingestible, controllable, and degradable origami robot for patching stomach wounds. In *2016 IEEE International Conference on Robotics and Automation (ICRA)*, volume 2016-June, pages 909–916. IEEE, may 2016. ISBN 978-1-4673-8026-3. doi: 10.1109/ICRA.2016.7487222. URL http://ieeexplore.ieee.org/document/7487222/.

Jaekwang Nam, Gun Hee Jang, Seung Mun Jeon, and Kyun Choi. Development of a Crawling Microrobot With High Steering Capability and High Stability to Navigate Through a Sharply Bent Tubular Environment. *IEEE Transactions on Magnetics*, 50(11):1–4, nov 2014. ISSN 0018-9464. doi: 10.1109/TMAG.2014.2324589. URL http://ieeexplore.ieee.org/document/6971625/.

Lan N. Pham and Jake J. Abbott. A Soft Robot to Navigate the Lumens of the Body Using Undulatory Locomotion Generated by a Rotating Magnetic Dipole Field. In *2018 IEEE/RSJ International Conference on Intelligent Robots and Systems (IROS)*, pages 1783–1788. IEEE, oct 2018. ISBN 978-1-5386-8094-0. doi: 10.1109/IROS.2018.8594247. URL https://ieeexplore.ieee.org/document/8594247/.

Lan N. Pham, Jake A. Steiner, Kam K. Leang, and Jake J. Abbott. Soft Endoluminal Robots Propelled by Rotating Magnetic Dipole Fields. *IEEE Transactions on Medical Robotics and Bionics*, 2(4):598–607, nov 2020. ISSN 2576-3202. doi: 10.1109/TMRB.2020.3027871. URL https://ieeexplore.ieee.org/document/9209999/.

Ziyu Ren, Rongjing Zhang, Ren Hao Soon, Zemin Liu, Wenqi Hu, Patrick R. Onck, and Metin Sitti. Soft-bodied adaptive multimodal locomotion strategies in fluid-filled confined spaces. *Science Advances*, 7(27), jul 2021. ISSN 2375-2548. doi: 10.1126/sciadv.abh2022. URL https://www.science.org/doi/10.1126/sciadv.abh2022.

Jake A. Steiner, Lan N. Pham, Jake J. Abbott, and Kam K. Leang. Modeling and Analysis of a Soft Endoluminal Inchworm Robot Propelled by a Rotating Magnetic Dipole Field. *Journal of Mechanisms and Robotics*, 14(5):1–11, oct 2022. ISSN 1942-4302. doi: 10.1115/1.4053114. URL https://asmedigitalcollection.asme.org/mechanismsrobotics/article/14/5/051002/1128866/Modeling-and-Analysis-of-a-Soft-Endoluminal.

Yingdan Wu, Xiaoguang Dong, Jae-kang Kim, Chunxiang Wang, and Metin Sitti. Wireless soft millirobots for climbing three-dimensional surfaces in confined spaces. *Science Advances*, 8(21), may 2022. ISSN 2375-2548. doi: 10.1126/sciadv.abn3431. URL https://www.science.org/doi/10.1126/sciadv.abn3431.

Changyu Xu, Zilin Yang, Shaun Wee Kiat Tan, Jianhuang Li, and Guo Zhan Lum. Magnetic Miniature Actuators with Six-Degrees-of-Freedom Multimodal Soft-Bodied Locomotion. *Advanced Intelligent Systems*, 4(4):2100259, 2022. ISSN 2640-4567. doi: 10.1002/aisy.202100259.

Qiji Ze, Shuai Wu, Jize Dai, Sophie Leanza, Gentaro Ikeda, Phillip C. Yang, Gianluca Iaccarino, and Ruike Renee Zhao. Spinning-enabled wireless amphibious origami millirobot. *Nature Communications*, 13(1):3118, dec 2022a. ISSN 2041-1723. doi: 10.1038/s41467-022-30802-w. URL https://www.nature.com/articles/s41467-022-30802-w.

Qiji Ze, Shuai Wu, Jun Nishikawa, Jize Dai, Yue Sun, Sophie Leanza, Cole Zemelka, Larissa S. Novelino, Glaucio H. Paulino, and Ruike Renee Zhao. Soft robotic origami crawler. *Science Advances*, 8(13):1–10, apr 2022b. ISSN 2375-2548. doi: 10.1126/sciadv.abm7834. URL https://www.science.org/doi/10.1126/sciadv.abm7834.